ON THE IMPLEMENTATION OF MOMENT TRANSPORT EQUATIONS IN OPENFOAM TO PRESERVE CONSERVATION, BOUNDEDNESS AND REALIZABILITY

ON THE IMPLEMENTATION OF MOMENT TRANSPORT EQUATIONS IN OPENFOAM TO PRESERVE CONSERVATION, BOUNDEDNESS AND REALIZABILITY

Antonio Buffo[a], Daniele L. Marchisio, Marco Vanni

[a] *DISAT, Politecnico di Torino, C.so Duca degli Abruzzi 24,10129, Torino, Italy Email: daniele.marchisio@polito.it*

ABSTRACT

Different industrial scale multiphase systems can be successfully described by considering their polydispersity (e.g. particle/droplet/bubble size and velocity distributions) and phase coupling issues are properly overcome only by considering the evolution in space and time of such distributions, dictated by the so-called Generalized Population Balance Equation (GPBE). A computationally efficient approach for solving the GPBE is represented by the quadrature-based moment methods, where the evolution of the entire particle/droplet/bubble population is recovered by tracking some specific moments of the distribution and the quadrature approximation is used to solve the "closure problem" typical of moment-based methods. In this contribution some crucial computational and numerical details concerning the implementation of these methods into the opensource Computational Fluid Dynamics (CFD) code OpenFOAM are discussed. These aspects are in fact very often overlooked, resulting in implementations that do not satisfy the properties of conservation, realizability and boundedness. These constraints have to be satisfied in a consistent way, with respect to what done with the other conserved transported variables (e.g. volume fraction of the disperse phase) also when higher-order discretization schemes are used. These issues are illustrated on examples taken on our work on the simulation of fluid-fluid multiphase systems.

1. INTRODUCTION

Turbulent particulate systems, such as fluid-fluid or solid-fluid are very common in the process industry. The design and the scale-up of vessels in which similar systems are present is currently performed by means of correlations based on experiments, with the important limitation that their validity is guaranteed only in specific vessel geometries and operating conditions close to those experimented. Moreover the empirical correlations consider only volume-averaged properties, neglecting the significant spatial inhomogeneities that characterize the behaviour of the industrial scale vessels.

Nowadays, Computational Fluid Dynamics (CFD) coupled with Population Balance Model (PBM) offers the possibility to overcome these issues and properly predict the behaviour of large scale equipment, considering that such systems are constituted by distribution of bubbles/drops/particles, namely they are polydisperse; the phase coupling issues and the mass transfer rates can be successfully described only if the existence of these distributions is properly accounted for, by considering a multidimensional Population Balance Equation

(PBE) that correctly treats the interactions between continuous fluid phase and the disperse particulate phase (e.g., coalescence, breakage, erosion, mass transfer, chemical reactions).

A very promising approach for solving this equation is represented by the Conditional Quadrature Method of Moments (CQMOM) due to its low computational demand. By using this method, the evolution in physical space and time of the relevant properties are recovered by considering some lower-order moments of the distribution. As pointed out in our previous works [1,2], it is essential to adopt proper submodels for describing the physics of such particulate systems, namely accurately evaluating the rates of the physical phenomena involved. However, another important aspect is represented by the implementation of this methodology in CFD codes, since the moments of the polydisperse distribution are conserved variables, bounded between physically reasonable values and expression of a possible realization of the system. To ensure these properties from the numerical point of view, it is appropriate to adopt specific measures in terms of implementation of the moment transport equation inside the CFD code, not easily or even impossible to apply in commercial codes. For this reason, the open source CFD code OpenFOAM is here used, considering also the appeal that nowadays open source frameworks have on both scientific and industrial communities.

This paper is structured as follows. First the governing equations are presented, showing the main features of CFD-PBM approach. Then the definition of the desired properties of moment conservation, boundedness and realizability are introduced and the numerical methods for ensuring them in a CFD code implementation are explained. In the last section, some test cases are eventually discussed.

2. MODEL DESCRIPTION

Let us consider a bubbly flow, with a continuous liquid phase and a disperse gas phase. The bubbles in a turbulent liquid can be thought of as a population evolving chaotically and being characterized by different properties, such as size L and chemical composition $\boldsymbol{\varphi}_\mathrm{b}$ (the so-called internal coordinates of the population, which are different from the external coordinate, namely the space and time). This population can be represented from the mathematical point of view by a smooth and differentiable function, the Number Density Function (NDF), obtained by ensemble averaging and defined as follows:

$$n(L,\boldsymbol{\varphi}_\mathrm{b};\mathbf{x},t)\,\mathrm{d}L\,\mathrm{d}\boldsymbol{\varphi}_\mathrm{b}\mathrm{d}\mathbf{x}\,, \tag{1}$$

namely the expected number of bubbles in the infinitesimal volume d$\mathbf{x}$, around the physical point $\mathbf{x}$, with the size of the bubbles in the range between L and L+dL and chemical composition between $\boldsymbol{\varphi}_\mathrm{b}$ and $\boldsymbol{\varphi}_\mathrm{b}$ + d$\boldsymbol{\varphi}_\mathrm{b}$. Of course, the number of internal coordinates could be increased in order to consider other properties of the distribution (e.g., bubble velocity, bubble temperature); however, in this work, only size and composition are taken into account. Within these assumptions, the system considered results in an isothermal gas-liquid dispersion with low gas hold-up, where the effects of bubble collision, coalescence and breakage on momentum exchange are neglected. Moreover, in this work, only two components are considered, nitrogen and oxygen, with only one transferring between phases (i.e., oxygen). For this reason, the chemical composition is here considered as a scalar φ_b, representing the number of moles of oxygen within one single bubble. Space and time dependencies will be omitted in the following in order to simplify the notation. Eventually it is important to stress that although the discussion is here focused on a bubbly gas-liquid flow, the conclusions are

more general and can be indeed extended to other fluid-fluid systems, as well as to particle-fluid systems.

As explained elsewhere [1-4], the continuity statement of the NDF leads to the Generalized Population Balance Equation (GPBE) and the solution of this multidimensional equation can be very demanding from the computational point of view. As previously mentioned, this aspect plays an important role, especially when the evolution of the NDF in the physical space is required. For this reason, the Conditional Quadrature Method of Moments (CQMOM) represent an attractive way to solve the GPBE. A generic moment of the NDF can be defined in the following way:

$$M_{k,l} = \int_{\Omega_L}\int_{\Omega_\varphi} n(L,\varphi_\mathrm{b})\, L^k \varphi_\mathrm{b}^l \,\mathrm{d}L\,\mathrm{d}\varphi_\mathrm{b}\,, \tag{2}$$

where Ω_l and Ω_φ represent the phase spaces of all the possible values of size and composition considered, while the indices k and l represent the order of the moments for each internal coordinates. Lower-order moments have important meaning from the engineering point of view: in fact, $M_{0,0}$ represents the total number density of bubbles per unit volume, $M_{1,0}$ represents the total bubble length density per unit volume, $M_{0,1}$ represents the total oxygen moles density in the bubbles per unit volume, $M_{2,0}$ is related to the total specific surface area per unit volume through the shape factor k_A, whereas $M_{3,0}$ is related to total volume fraction through the volumetric shape factor k_V.

By applying the moment transform to the GPBE, it is possible to write the following statement [1]:

$$\frac{\partial M_{k,l}}{\partial t} + \frac{\partial}{\partial \mathbf{x}}\cdot\left(M_{k,l}\,\mathbf{u}_{k,l}\right) = H_{k,l}\left(L,\varphi_\mathrm{b}\right) + \int_0^\infty k L^k G\, n\left(L,\varphi_\mathrm{b}\right)\mathrm{d}L + \int_0^\infty l\varphi_\mathrm{b}^l\, \dot{\varphi}_\mathrm{b}\, n\left(L,\varphi_\mathrm{b}\right)\mathrm{d}\varphi_\mathrm{b}\,, \tag{3}$$

where G is the rate of continuous change of bubble size, related to molecular process (e.g., evaporation, condensation, mass transfer), $\dot{\varphi}_\mathrm{b}$ is the rate of continuous change of bubble composition (with respect to the different chemical components) related to reactive or mass transfer process and $\mathbf{u}_{k,l}$ is the velocity of the moment of order k,l, different for each generic moment of the NDF. The right hand side term of Eq. (3) models the discontinuous events, accounting the instantaneous change of $M_{k,l}$ due to bubble collision, coalescence and breakage. It is important to remark that the Eq. (3) is closed, without assuming a functional form of NDF, only in the unrealistic case when $\mathbf{u}_{k,l}$, G, $\dot{\varphi}_\mathrm{b}$, as well as coalescence and breakage frequencies are independent from the state of the disperse phase. In realistic cases, the closure problem is overcome through the assumption of the following functional form for the NDF, typical of the CQMOM approach[4]:

$$n(L,\varphi_\mathrm{b}) = \sum_{i=1}^{N_1} w_i\,\delta\left(L - L_i\right)\sum_{j=1}^{N_2} w_{i,j}\,\delta\left(\varphi_\mathrm{b} - \varphi_{\mathrm{b};i,j}\right), \tag{4}$$

where the number density $w_{i,j}$ and the composition $\varphi_{i,j}$ are values calculated on the first internal coordinate L_i with number density w_i. The number densities are usually referred as weights of quadrature, instead the internal coordinate values are called nodes or abscissas of quadrature [2]. By calculating the weights and nodes of quadrature through the so-called CQMOM inversion algorithm it is possible to close the Eq. (3), since now we are able to evaluate all the integrals appearing on the right hand side of the equation. It is worth mentioning that the total number of quadrature nodes is equal to $N = N_1 \cdot N_2$, where N_1 is the

number of nodes used to approximate the multivariate NDF with respect to the bubble size and N_2 is the number of nodes with respect to bubble composition. Each one of the N_1 groups of bubbles, characterized by size L_i is subdivided in N_2 group of bubbles characterized by composition equal to $\varphi_{b;i,j}$. It is interesting to notice that a preliminary choice related to the order of the internal coordinates has to be made. This decision depends on the problem under study: in this particular case, bubble size is selected as first and then bubble composition is selected as second. Moreover, N_1 is here assumed equal to 2 and N_2 equal to 1. For details on the CQMOM inversion algorithm see [1,4].

2.1 Population Balance Modeling and CFD

The definition of the different terms appeared in Eq. (3) is needed to solve the GPBE. The expressions of G_i and $\dot{\varphi}_{b;i}$ are formulated by considering only the effect of oxygen mass transfer, through a simple mass balance on a single bubble:

$$G_i = \frac{2k_L M_w}{\rho_b}\left(\psi_c - H_{O_2}\frac{\phi_{b;i}}{k_V L_i^3}\right), \qquad \dot{\phi}_{bi} = \frac{6k_L}{L_i}\left(\psi_c - H_{O_2}\frac{\phi_{b;i}}{k_V L_i^3}\right), \tag{11}$$

where M_w is the molecular weight of oxygen, ψ_c is the concentration of oxygen in the continuous phase and H_{O_2} is the Henry constant . To estimate the mass transfer coefficient k_L, the correlation of Lamont and Scott [5], based on local value of the turbulent dissipation rate epsilon was used here. Moreover, it is important to remind that as a result of considering N_2 = 1 for CQMOM, it is equivalent to write $\varphi_{b;i,j} = \varphi_{b;i}$ and $w_i = w_i \cdot w_{i,j}$.

From the theory of coalescence and breakage [6] it is possible to define the source term of Eq.(3), and for the sake of brevity we report here only the final form:

$$H_{k,l}^{(N)} = \frac{1}{2}\sum_{i=1}^{N}\sum_{j=1}^{N} w_i w_j h_{i,j}[(L_i^3 + L_j^3)^{k/3}(\phi_{b;i} + \phi_{b;j})^l - L_i^k \phi_{b;i}^l - L_j^k \phi_{b;j}^l] + \sum_{i=1}^{N} w_i \beta_i [P_{k,l}^{(i)} - L_i^k \phi_{b;i}^l], \tag{12}$$

where $h_{i,j}$ is the coalescence kernel, β_i is the breakage kernel and $P_{k,l}^{(i)}$ is the generic moment of the daughter distribution function. For the formulation of these terms, readers may refer to the literature (for details see [1,7]).

The calculation of the advection term $\mathbf{u}_{k,l}$ of the transport equation for a generic moment $M_{k,l}$ requires the knowledge of the bubble velocity field. This information can be recovered by using the Eulerian-Eulerian multi-fluid approach usually implemented in CFD codes, through the following governing equations:

$$\frac{\partial \rho_i \alpha_i}{\partial t} + \frac{\partial}{\partial \mathbf{x}} \cdot (\rho_i \alpha_i \mathbf{u}_i) = \Gamma_i, \tag{13}$$

$$\frac{\partial \rho_i \alpha_i \mathbf{u}_i}{\partial t} + \frac{\partial}{\partial \mathbf{x}} \cdot (\rho_i \alpha_i \mathbf{u}_i \mathbf{u}_i) = -\nabla \cdot (\alpha_i \boldsymbol{\tau}_i) - \alpha_i \nabla p + \rho_i \alpha_i \mathbf{g} + M_i, \tag{14}$$

where $\boldsymbol{\tau}_i$ is the tensor accounting for both viscous and turbulent stresses, p is the pressure field shared between all the phases, **g** is the gravity, Γ_i and M_i are respectively the mass and momentum exchange term between phase *i* and all the other phases present in the system. It can be shown that Eqs. (13) and (14) can be also derived from the GPBE (for details see **[**1,3**]**). The *i* index stands for both continuous and disperse phases, and more than two different phases can be considered. In gas-liquid modelling, it is common to assume one

continuous liquid phase with volume fraction α_c and velocity $\mathbf{u}_c$ and N disperse gas phases with volume fraction $\alpha_{b;i}$, size L_i, chemical composition $\phi_{b;i}$ and velocity $\mathbf{u}_{b;i}$. In this case, M_i is the force per unit volume acting on a group of bubbles with size L_i that can be modelled in the following way, considering only the drag force:

$$M_i = \frac{3}{4}\frac{\alpha_c C_{D;i}\rho_c}{L_i}\left\|\mathbf{u}_{r;i}\right\|\left(\mathbf{u}_{r;i}\right) \tag{15}$$

where $\mathbf{u}_{r;i} = \mathbf{u}_c - \mathbf{u}_{b;i}$ is the slip velocity, namely the velocity difference between continuous phase and the disperse phase characterized by bubbles with size L_i. Moreover, the volume fraction of i-th gas phase can be expressed as function of the quadrature approximation as follows [8]:

$$\alpha_{b;i} = k_V w_i L_i^3 . \tag{16}$$

As evident in Eqs. (14) and (15), in this work only the drag, gravity and buoyancy forces are considered for the sake of simplicity; however other contributions can be easily accounted for (i.e., virtual mass or lift). For calculating the drag coefficient $C_{D;i} = C_D(L_i)$, the approach proposed by Petitti *et al.* [9], based on the terminal bubble velocity in a stagnant liquid with a proper correction that consider the effect of other bubbles and the effect of turbulence was here adopted. As far as the velocity of a generic moment $M_{k,l}$ is concerned, it is possible to write the following relation:

$$\mathbf{u}_{k,l} = \sum_{i=1}^{N} p_{k,l;i}\mathbf{u}_{b;i} \text{ , where } p_{k,l;i} = \frac{w_i L_i^k \varphi_{b;i}^l}{M_{k,l}} . \tag{17}$$

Another common assumption, here adopted, is to consider a unique disperse gas phase, since bubbles in a range between 2-10 mm have more or less the same terminal velocity. In this case, the gas volume fraction α_b can be written in function of the moments in the following way:

$$\alpha_b = k_V M_{3,0}, \tag{18}$$

while the moment velocity $\mathbf{u}_{k,l}$ is equal to the bubble velocity $\mathbf{u}_b$ according to Eq. (17).

3. MOMENT BOUNDEDNESS, REALIZABILITY AND CONSERVATION

By definition, the gas volume fraction α_b is a quantity bounded between 0 and 1. As a consequence of this fact, also the moment of order three with respect to the bubble size is bounded between 0 and a maximum value dictated by Eq. (18). In general, since the moments represent physical quantities, the values of all moments are limited between a minimum and a maximum value. As we will see in the following, it is possible to ensure the boundedness of moments through a specific numerical scheme, derived from the scheme for the volume fraction α_b proposed by Oliveira and Issa [10].

In addition to this important property, the moment set transported has to be realizable, namely the quadrature weights and abscissas underlying the moment set have to be positioned in allowed portion of the phase spaces. When this situation is not verified, we are in front of the so-called "moment corruption" problem. A unrealizable moment set leads to wrong or even unphysical values for weights and abscissas of the quadrature approximation when the CQMOM algorithm is applied, jeopardizing not only the accuracy but also the stability of the

simulation. It was demonstrated that a spatial discretization scheme for the moments of order higher than the first order upwind may result to unrealizable moment set [11]. However, also in this case, it is possible to prevent this unwanted situation by using specific spatial discretization schemes for the moments [12]. In this work, we will see how to combine these two schemes in order to guarantee moment boundedness and realizability.

3.1 Numerical scheme to ensure moment boundedness

The governing equations for the gas volume fraction and for his complement, the liquid volume fraction, considering both phases as incompressible, follow from Eq. (13) and can be written in the following way:

$$\frac{\partial \alpha_b}{\partial t} + \frac{\partial}{\partial \mathbf{x}} \cdot \left(\alpha_b \mathbf{u}_b\right) = \frac{\Gamma_b}{\rho_b}, \qquad \frac{\partial \alpha_c}{\partial t} + \frac{\partial}{\partial \mathbf{x}} \cdot \left(\alpha_c \mathbf{u}_c\right) = \frac{\Gamma_c}{\rho_c}, \tag{19}$$

and together with the two conditions $\alpha_b+\alpha_c=1$ and $\Gamma_b+\Gamma_c=0$, Eqs, (19) guarantee that the total mass of the gas-liquid system is properly conserved. By summing the two equations, the following expression is obtained:

$$\frac{\partial}{\partial \mathbf{x}} \cdot \left(\mathbf{u}_{vm}\right) = \frac{\Gamma_b}{\rho_b} - \frac{\Gamma_b}{\rho_c}, \tag{20}$$

where $\mathbf{u}_{vm}= \alpha_b\mathbf{u}_b +\alpha_c\mathbf{u}_c$ is the mean volumetric velocity, and Eq. (20) tells us that its field is divergence free if there is no mass transfer. In two-fluid CFD codes, usually only the first equation of Eqs (19) is solved and the volume fraction of the continuous phase α_c is calculated as $1 - \alpha_b$; however, if the equation for α_b is implemented as written in Eqs. (19), the boundedness of the gas volume fraction between zero and one may not be ensured from the numerical point of view. Starting from the definition of mean volumetric velocity $\mathbf{u}_{vm}= \alpha_b\mathbf{u}_b +\alpha_c\mathbf{u}_c$ and relative velocity $\mathbf{u}_r= \mathbf{u}_c - \mathbf{u}_b$, it is possible to write:

$$\mathbf{u}_b = \mathbf{u}_{vm} - \alpha_c \mathbf{u}_r = \mathbf{u}_{vm} - (1-\alpha_b)\mathbf{u}_r, \tag{21}$$

and by substituting this expression in the first equation of Eqs (19), after some manipulations the following equation is obtained [10]:

$$\frac{\partial \alpha_b}{\partial t} + \alpha_b \frac{\partial}{\partial \mathbf{x}} \cdot \left(\mathbf{u}_{vm}\right) + \mathbf{u}_{vm} \cdot \frac{\partial}{\partial \mathbf{x}} \left(\alpha_b\right) - \frac{\partial}{\partial \mathbf{x}} \cdot \left(\alpha_b (1-\alpha_b)\mathbf{u}_r\right) = \frac{\Gamma_b}{\rho_b}. \tag{22}$$

In case of no mass transfer (i.e., $\Gamma_b = 0$), it is clearly possible to observe that the implementation reported in Eq. (22) is capable of preserving the boundedness of the gas volume fraction: in fact, the second term is equal to zero according to Eq. (20), the third term is an amplitude preserving the wave transport term and the fourth term guarantees that $0 \leq \alpha_b \leq 1$ since it goes to zero at both limits. Otherwise, in case of mass transfer, Eq. (22) can be rewritten in order to include Eq. (20) in the following manner:

$$\frac{\partial \alpha_b}{\partial t} + \mathbf{u}_{vm} \cdot \frac{\partial}{\partial \mathbf{x}} \left(\alpha_b\right) - \frac{\partial}{\partial \mathbf{x}} \cdot \left(\alpha_b (1-\alpha_b)\mathbf{u}_r\right) = (1-\alpha_b)\frac{\Gamma_b}{\rho_b} + \alpha_b \frac{\Gamma_b}{\rho_c}, \tag{23}$$

where the advective terms still preserve the boundedness of the volume fraction.

Since the gas volume fraction α_b is proportional to the moment of order three with respect to bubble size $M_{3,0}$ according to the Eq. (18), it is evident that a similar idea for preserving

boundedness can be applied also to the moment transport equation. By collecting all the source term of Eq.(3) in a unique source term $S_{k,l}$ and assuming that all the moments move in the physical space with the same velocity $\mathbf{u}_b$, it is possible to write the following transport equation for a generic order moment:

$$\frac{\partial M_{k,l}}{\partial t} + \frac{\partial}{\partial \mathbf{x}} \cdot \left(M_{k,l} \mathbf{u}_b \right) = S_{k,l} , \tag{24}$$

which has the form of a generic partial differential equation with source term. However, as we will see in the following, a similar implementation is not capable of preserving the boundedness of the moments; instead, by substituting the bubble velocity $\mathbf{u}_b$ according to the Eq. (21), the following expression similar to Eq. (22) can be written:

$$\frac{\partial M_{k,l}}{\partial t} + \frac{\partial}{\partial \mathbf{x}} \cdot \left(M_{k,l} \mathbf{u}_{vm} \right) - \frac{\partial}{\partial \mathbf{x}} \cdot \left(M_{k,l} (1 - \alpha_b) \mathbf{u}_r \right) = S_{k,l} , \tag{25}$$

where the gas volume fraction can be substituted by using the Eq. (18), leading to what follows:

$$\frac{\partial M_{k,l}}{\partial t} + M_{k,l} \frac{\partial}{\partial \mathbf{x}} \cdot \left(\mathbf{u}_{vm} \right) + \mathbf{u}_{vm} \cdot \frac{\partial}{\partial \mathbf{x}} \left(M_{k,l} \right) - \frac{\partial}{\partial \mathbf{x}} \cdot \left(M_{k,l} (1 - k_V M_{3,0}) \mathbf{u}_r \right) = S_{k,l} , \tag{26}$$

where the second term is equal to zero in case of no mass transfer. Otherwise, in case of mass transfer, it is possible to demonstrate that $\Gamma_b = k_V \rho_b S_{3,0}$ (where $S_{3,0}$ is the source term of the moment of order three with respect to bubble size) and after some algebraic manipulations, Eq. (26) becomes:

$$\frac{\partial M_{k,l}}{\partial t} + \mathbf{u}_{vm} \cdot \frac{\partial}{\partial \mathbf{x}} \left(M_{k,l} \right) - \frac{\partial}{\partial \mathbf{x}} \cdot \left(M_{k,l} (1 - k_V M_{3,0}) \mathbf{u}_r \right) = S_{k,l} - M_{k,l} k_V S_{3,0} \left(1 - \frac{\rho_b}{\rho_c} \right) . \tag{27}$$

As we will see in the following sections, this implementation is capable of ensuring the boundedness of the moments. Moreover, it can be shown that the transport equation of the moment $M_{3,0}$ and the volume fraction α_b are equivalent from the mathematical point of view (the demonstration is not reported here for the sake of brevity).

3.2 Numerical scheme to ensure moment realizability

It is useful to remark here that a moment set is valid if there exists an NDF resulting in that specific moment set: in this way, the quadrature is realizable, namely the calculated abscissas are always in the domain of the phase space and the weights are always positive. Otherwise, when the inversion algorithm is used with an invalid moment set, unrealizable quadratures are calculated, because no realizable NDF corresponds to an invalid set, ruining the accuracy and the stability of the simulation.

As previously mentioned, the generation of corrupted moment sets may arise when high-order spatial discretization schemes are used for transporting the moments of the NDF [11]. This is due to the fact that the interpolation scheme for moment values at the face between two neighbouring cells may result in a unrealizable moment set, and this corrupted set may propagate rapidly in the computational domain, since the interpolation at the cell faces is used when the advective term of moment transport equation is calculated by the code. In a recent work, an iterative algorithm was proposed to correct a corrupted moment set based on the

convexity principle [11], but this algorithm is only capable to restore the set, not to prevent and definitely solve the corruption problem.

Very recently a class of high-order numerical schemes was introduced [12], based on the kinetic finite volume schemes, that guarantees the realizability of a set of moments. This class of discretization schemes is based on the idea of interpolating at the faces of the cells the values of quadrature weights and abscissas instead of the moments themselves: in this way, it is possible to build discretization schemes that always prevent the rise of moment corruption problem. In particular, it is possible to demonstrate that the moment set is always realizable when the abscissas are interpolated by using the first order upwind and the weights are interpolated with higher order schemes, providing that the time step used follows some specific constraints (for details, see the original work [12]). Moreover, it is also possible to prove that it is mathematically equivalent to use the first order upwind for both weights and abscissas or to directly interpolate the moment themselves with the first order upwind [CITE]; for this reason we always used the first order upwind for the moments equation in our previous works, both on commercial and opensource CFD codes [1,3,4].

In this work, we coupled the implementation for ensuring boundedness (i.e., Eq. (27)) with the interpolation strategy for ensuring realizability of the moment set. This means that, at the beginning of every time step, the moment set in every cell of the domain is inverted with the CQMOM algorithm in order to find the quadrature weights and abscissas, then the value of the moments at the faces of the cells are calculated from the interpolated weights and abscissas, the former obtained with an high order method (i.e., second order upwind) and the latter with the first order upwind, finally the advective and the source terms of Eq. (27) are calculated and the equations for the moments are solved.

4. TEST CASE, RESULTS AND DISCUSSION

The geometry considered as a test case is a two-dimensional partially aerated bubble column, with the inlet located in the middle of the bottom. The grid is constituted by a limited number

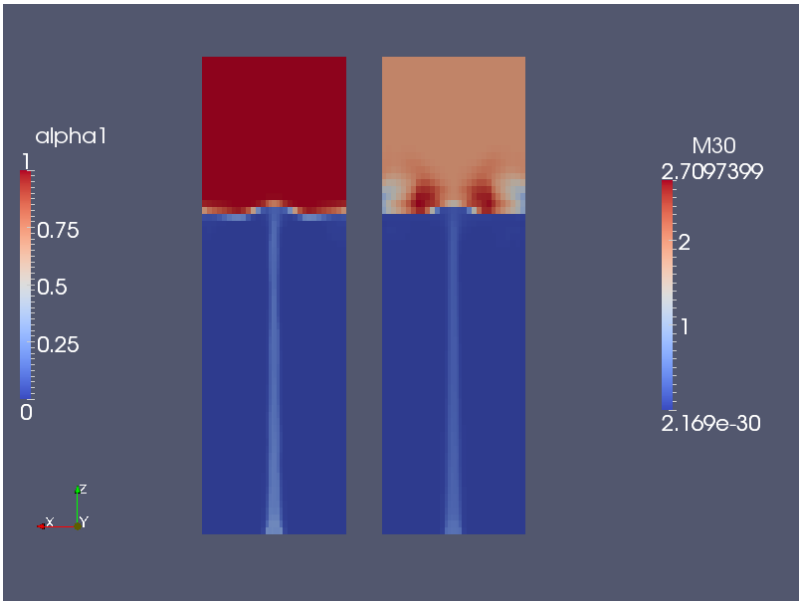

Figure 1. Instantaneous contour plots of α_b (left) and $M_{3,0}$ (right) at t = 2 s for the case in which the moment transport equations are implemented by using Eq. (24)

of rectangular non-uniform cells (32x70), in order to enhance the effects of numerical diffusion. The simulated gas superficial velocity corresponds to 5 mm/s, which is a realistic velocity for a bubble column working in the homogeneous regime. All the simulations performed are transient with a time step equal to 0.001 s: at the initial time, the interface between the gas and liquid is located a two third of the column. For a detailed discussion on boundary conditions for such system, see [3]. The standard OpenFOAM solver for Eulerian-Eulerian incompressible two-fluid systems is modified in order to include the population balance model: different solvers are created for considering different implementations of the moment transport equations. Details on the models used for bubble coalescence and breakup rates can be found in our previous works [1,4]. The following test cases are here carried out: firstly the moments are transported by using Eq. (24) without ensuring boundedness with the first order upwind as a discretization scheme, then by using Eq. (27) ensuring boundedness with the first order upwind as a discretization scheme and finally by using Eq. (27) with different discretization schemes for weights and nodes of the quadrature approximation (second order upwind for the weights and first order upwind for the nodes).

In Figure 1, the instantaneous contour plots for the gas volume fraction and the moment of order three with respect to bubble size are reported for t = 2 s for the case in which the moments are transported by using Eq. (24) without ensuring boundedness with the first order upwind. As it is possible to notice, the values of the gas volume fraction are bounded between zero and one, since Eq. (23) that guarantees the boundedness of α_b is used, whereas the values reached in some cells of the domain by the moment of order three are higher than $M_{3,0} = \alpha_b / k_V = 6 / \pi \sim 1.90986$. It is worth mentioning that the moments of the bubble distribution are not defined when the gas becomes the continuous phase above the interface; however, since the equations of the moments are solved for all the domain and the realizability of the moment sets must be preserved for the stability of the simulation, this situation is not acceptable.

In Figure 2, the instantaneous contour plots for the gas volume fraction and the moment of order three with respect to bubble size are reported for t = 2 s for the case in which the

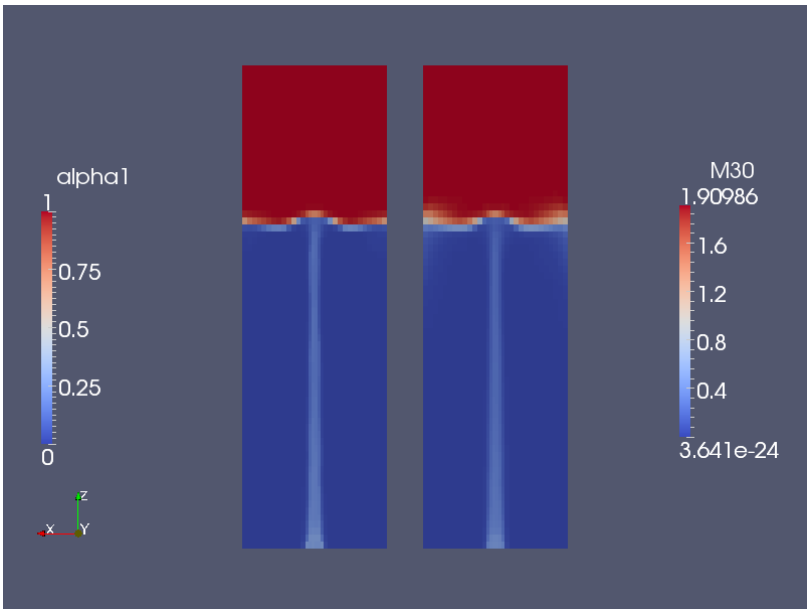

Figure 2. Instantaneous contour plots of α_b (left) and $M_{3,0}$ (right) at t = 2 s for the case in which the moment transport equations are implemented by using the preseriving boundedness scheme reported in Eq. (27)

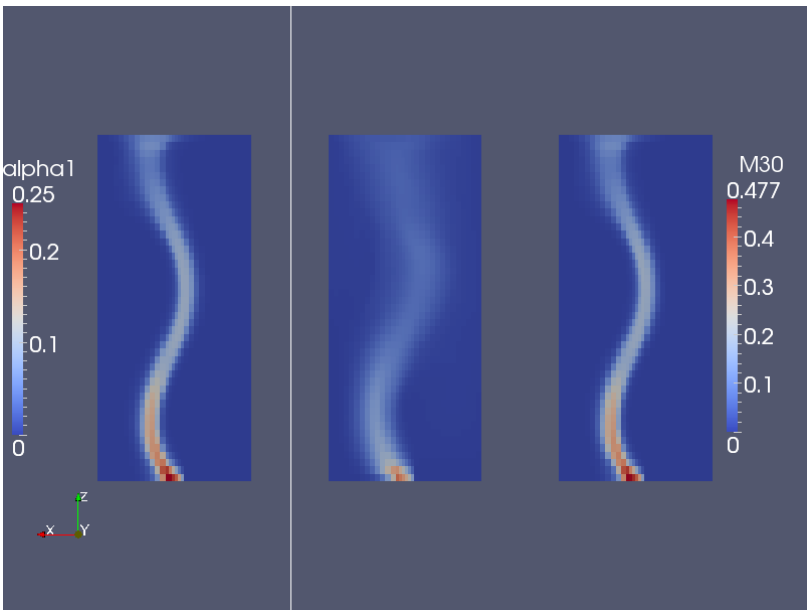

Figure 3. Instantaneous contour plots of α_b (left) and $M_{3,0}$ at t = 100 s for the case in which the moment transport equations are implemented by using the preserving boundedness scheme reported in Eq. (27). The centre figure is obtain when first order upwind is used, instead at right the realizable high order discretization scheme for the moment equations. Only the domain under the liquid level is visualized.

moments are transported by using Eq. (27), with the numerical implementation that ensures boundedness of the moment values by using the first order upwind as discretization scheme. In this case, it is possible to see that the two contour plots are similar as expected: $M_{3,0}$ is now bounded between values corresponding to α_b= 0 and α_b= 1. The differences in the two contour plots are in this case due to the different discretization schemes used for the volume fraction (blended upwind scheme with van Leer slope limiter) and $M_{3,0}$ (first order upwind); in fact the solution of α_b is less diffusive than $M_{3,0}$, since a lower order scheme is used for the moments on a very coarse grid. Further simulation on a refined mesh showed (results here are not reported for the sake of brevity) that the difference between the two fields significantly reduces.

In Figure 3, the comparison between the first order upwind and a realizable high order discretization schemes in terms of moment of order three with respect to bubble size is reported for t = 100 s. It is clear that the numerical diffusion plays an important role in this test case: the solution obtained with the first order upwind is more diffusive than the realizable high order discretization scheme. For this case, the contour plot of $M_{3,0}$ is very similar to the profile of gas volume fraction for which it is valid the proportionality relationship, since the equation of α_b is solved by means of a high order scheme (blended upwind scheme with van Leer slope limiter).

5. CONCLUSIONS

In this work, the problem of moment conservation, boundedness and realizability is considered. These aspects are closely connected to often overlooked numerical details concerning the implementation of Method of Moments into the Computational Fluid Dynamics (CFD) codes. Since these constraints have to be satisfied in a consistent way, a new numerical approach is proposed, based on what usually is done with the other conserved

transported variables, as the volume fraction of the disperse phase. This methodology can be also adapted for use with realizable higher-order discretization schemes. A simplified geometry was used as the test case for three different numerical implementations of the moment transport equation, which were solved with the open source CFD code OpenFOAM. The analysis of the results shows that the proposed numerical approach is capable of preserving the boundedness and the realizability of the moment set and the stability of the code is assured. When a realizable higher order discretization scheme is used for the moments, the numerical diffusion of the solution is significantly reduced, allowing to use a coarser grid and therefore decreasing the computational costs.

REFERENCES

1. Buffo A., Marchisio D.L., (2014). Modeling and simulation of turbulent polydisperse gas-liquid systems via the Generalized Population Balance Equation, *Reviews in chemical Engineering*, **30**, 73-126.

2. Marchisio D.L., Fox R.O., (2013). *Computational Models for Polydisperse Particulate and Multiphase Systems*, Cambridge University Press, Cambridge.

3. Buffo A., Marchisio D.L., Vanni M., Renze P., (2013). Simulation of polydisperse multiphase systems using population balances and example application to bubbly flows, *Chemical Engineering Research & Design*, **91**, 1859-1875.

4. Buffo A., Vanni M., Marchisio D. L., Fox R. O., (2013). Multivariate Quadrature-Based Moments Methods for turbulent polydisperse gas-liquid systems, *International Journal of Multiphase Flow*, **50**, 41-57.

5. Lamont, J.C. and Scott, D.S., (1970). An eddy cell model of mass transfer into the surface of a turbulent liquid, *AICHE Journal*, **16**, 513–519.

6. Marchisio, D.L., Virgil, R.D., Fox, R.O., (2003b). Quadrature method of moments for aggregation-breakage processes, *Journal of Colloid and Interface Science*, **258**, 322–334.

7. Laakkonen, M., Alopaeus, V., Aittamaa, J., (2006). Validation of bubble breakage, coalescence and mass transfer models for gas-liquid dispersion in agitated vessel, *Chemical Engineering Science*, **61**, 218–228.

8. Buffo A., Vanni M., Marchisio D.L. (2012) Multidimensional population balance model for the simulation of turbulent gas-liquid systems in stirred tank reactors, *Chemical Engineering Science*, **70**, 31- 44.

9. Petitti M., Nasuti A., Marchisio D.L., Vanni M., Baldi G., Mancini N., Podenzani F. (2010) Bubble Size Distribution Modeling in Stirred Gas-Liquid Reactors with QMOM Augmented by a New Correction Algorithm, *AIChE Journal*, **56**, 36-53.

10. Oliveira P.J. Issa R.I., (2003). Numerical aspects of an algorithm for the Eulerian simulation of two-phase flows, *International Journal for Numerical Methods in Fluids*, **43**, 1177-1198.

11. Wright Jr. D.L., (2007). Numerical advection of moments of the particle size distribution in Eulerian models, *Journal of Aerosol Science*, **38**, 352-369.

12. Vikas V., Wang Z.J., Passalacqua A., Fox R.O., (2011). Realizable high-order finite volume schemes for quadrature-based moment methods, *Journal of Computational Physics*, **230**, 5328-5352.

13. Desjardins O., Fox R.O., Villedieu P., (2008). A quadrature-based moment method for dilute fluid-particle flows, *Journal of Computational Physics*, **227**, 2514-2539.